Eur J Nucl Med Mol Imaging (2016) 43:1646–1652
DOI 10.1007/s00259-016-3351-3

ORIGINAL ARTICLE

^{18}F-FDG PET/MRI evaluation of retroperitoneal fibrosis: a simultaneous multiparametric approach for diagnosing active disease

Verena Ruhlmann[1] · Thorsten Dirk Poeppel[1] · Alexander Sascha Brandt[2] · Johannes Grüneisen[3] · Marcus Ruhlmann[1] · Jens Matthias Theysohn[3] · Michael Forsting[3] · Andreas Bockisch[1] · Lale Umutlu[3]

Received: 14 January 2016 / Accepted: 18 February 2016 / Published online: 11 March 2016

Abstract
Purpose The aim of this study was to evaluate integrated ^{18}F-FDG PET/MRI as a one-stop diagnostic procedure in the assessment of (active) idiopathic retroperitoneal fibrosis (RPF)
Methods A total of 22 examinations comprising a PET/CT scan followed by a PET/MRI scan in 17 patients (13 men, 4 women, age 58 ± 11 years) with histopathologically confirmed RPF at diagnosis or during follow-up under steroid therapy were analysed in correlation with laboratory inflammation markers (ESR, CRP). The patient cohort was subdivided into two groups: 6 examinations in untreated and 16 in treated patients. Tissue formations in typically periaortic localization suggestive of RPF were visually and quantitatively evaluated. The PET analysis included the assessment of SUVmax and a qualitative score for FDG uptake in RPF tissue in relation to the uptake in the liver. MRI analysis included evaluation of the T2-weighted image signal intensity, contrast enhancement and diffusion restriction (ADC values). Mean values were compared using the Mann-Whitney *U* test. ADC, SUVmax and ESR values were correlated using Pearson's correlation.
Results MRI analysis revealed restricted diffusion in 100 % and 56 %, hyperintense T2 signal in 100 % and 31 %, and contrast enhancement in the periaortic tissue formation suggestive of RPF in 100 % and 62.5 % in the untreated and treated patients, respectively. In the qualitative and quantitative PET analysis, statistically significant differences were found for mean FDG uptake scores (2.5 ± 0.8 in untreated patients and 1.1 ± 0.9 in treated patients) and mean SUVmax (7.8 ± 3.5 and 4.1 ± 2.2, respectively). A strong correlation was found between the ADC values and SUVmax (Pearson r −0.65, P = 0.0019), and between ESR and CRP values and SUVmax (both r = 0.45, P = 0.061).
Conclusion Integrated ^{18}F-FDG PET/MRI shows high diagnostic potential as a one-stop diagnostic procedure for the assessment of (active) RPF providing multiparametric supportive information.

Keywords Retroperitoneal fibrosis · PET/MRI · Multiparametric · One-stop diagnostic procedure

Introduction

Retroperitoneal fibrosis (RPF) is an uncommon disease that presents as retroperitoneal proliferation of fibrous tissue surrounding the retroperitoneal vascular structures and potentially leading to vessel or ureteral obstruction, the most frequent complication of RPF [1–3]. Early clinical findings of RPF are nonspecific and include symptoms of chronic back pain, lower extremity oedema, and deep vein thrombosis [3]. Medical treatment is classically based on steroids to suppress the inflammatory activity [3, 4].

Diagnosis and management of RPF remains challenging due to a lack of standardized diagnostic criteria for idiopathic

✉ Verena Ruhlmann
verena.ruhlmann@uk-essen.de

[1] Department of Nuclear Medicine, Medical Faculty, University Duisburg-Essen, University Hospital Essen, Hufelandstraße 55, 45147 Essen, Germany

[2] Department of Urology and Paediatric Urology, HELIOS Medical Center Wuppertal, University Hospital Witten/Herdecke, Heusnerstr. 40, 42283 Wuppertal, Germany

[3] Department of Diagnostic and Interventional Radiology and Neuroradiology, University Hospital Essen, University Duisburg-Essen, Hufelandstraße 55, 45122 Essen, Germany

RPF and the nonspecific nature of the symptoms and laboratory markers. Hence, imaging is assigned an important role in diagnosis. While CT and MR imaging are considered the gold-standards for morphological evaluation of RPF [3, 5], the assessment of disease activity has grown to be the key for individual therapy management [6, 7]. Functional MRI, by means of dynamic contrast-enhanced MRI as well as diffusion-weighted imaging (DWI), has demonstrated its strong diagnostic potential for evaluation of disease activity [7–10]. Due to its excellent sensitivity for assessment of hypermetabolic activity, PET is well established in the diagnosis of oncological and infectious diseases, including RPF [3, 11–15]. Numerous studies have demonstrated its high diagnostic potential for assessment and quantification of active RPF, therapy monitoring and relapse detection, providing superior predictive markers for posttreatment prognosis compared with solely morphological CT or MR imaging [16, 17].

With the increasing implementation of integrated whole-body PET/MR devices, combining the strength of morphological and functional MRI as well as metabolic PET assessment, the aim of our study was to evaluate the diagnostic potential of integrated ^{18}F-FDG PET/MRI as a one-stop diagnostic procedure in the assessment of (active) idiopathic RPF.

Materials and methods

Study protocol

The study was approved by the local institutional review board and written informed consent was obtained from all patients before each examination. A total of 17 patients (13 men, 4 women, age 58 ± 11 years) with histopathologically confirmed idiopathic RPF at diagnosis or during follow-up under therapy underwent a clinically indicated whole-body ^{18}F-FDG PET/CT scan. After providing written consent, all patients were prospectively enrolled for a subsequent whole-body PET/MRI scan.

A total of 22 examinations comprising a non-contrast-enhanced, low-dose ^{18}F-FDG PET/CT scan followed by a PET/MRI scan were performed. These included 6 examinations in untreated patients with newly diagnosed disease and 16 examinations in patients under/after medical (steroid) therapy (seven examinations after 52 weeks of steroid therapy with four discontinuing prior to PET, and nine axaminations after further discharging of 54 weeks the steroid therapy). Parallel to each examination, erythrocyte sedimentation rate (ESR) and C-reactive protein (CRP) levels were also determined.

PET/CT imaging

Whole-body ^{18}F-FDG PET/CT scans were obtained on a Biograph™ PET/CT system (Siemens Molecular Imaging, Hoffmann Estates, IL). Prior to imaging, patients fasted for at least 6 h. All patients had blood glucose levels below 150 mg/dL at the time of ^{18}F-FDG injection. A total of 300 ± 64 MBq of ^{18}F-FDG was intravenously injected 60 ± 5 min before the scan. The low-dose CT scan without contrast enhancement was performed with the following parameters: caudocranial scan direction, field of view skull base to upper thighs, 110 kV, 15 mAs, slice thickness 5 mm, increment 2.4 mm. The PET scan parameters were as follows: 3-D mode, 3.5 min emission time per bed position, reconstruction according to the attenuation-weighted ordered-subsets expectation maximization (AW-OSEM) iterative algorithm with two iterations and eight subsets, gaussian filter with 5.0 mm full-width at half-maximum (FWHM) and scatter correction.

PET/MR imaging

Abdominal PET/MRI scans were then performed 140 ± 41 min after tracer injection on an integrated 3.0-T hybrid PET/MR system (Biograph mMR; Siemens Healthcare GmbH, Erlangen, Germany). PET datasets were acquired in two bed positions (axial field of view 25.8 cm, 5 min per bed position) with an acquisition time of 5 min each covering the lower thorax to the pelvis with a 344 × 344 matrix and a gaussian filter with 4 mm FWHM. MRI datasets were acquired simultaneously using phased-array body surface coils. The PET data were reconstructed in 3-D mode using ordinary Poisson OSEM with three iterations and 21 subsets. Attenuation correction was based on an automatically generated four-compartment model attenuation map (μ-map) derived from a two-point T1-weighted (T1-W) Dixon VIBE (volumetric interpolated breath-hold examination) sequence [18].

The MRI protocol comprised the following sequences: a transverse non-enhanced T1-W and transverse non-enhanced T2-weighted (T2-W) half Fourier-acquired single shot turbo spin echo (HASTE) sequence with fat saturation, DWI with b-values of 0, 500 and 1,000 s/mm^2 with in-line reconstruction of apparent diffusion coefficient (ADC) maps, transverse contrast-enhanced, fat-saturated T1-W VIBE sequence after intravenous administration of 0.1 mmol/kg body weight of gadobutrol (Gadovist; Bayer Healthcare, Germany) and a transverse T2-W fast low-angle shot (FLASH) sequence. The average acquisition time of the PET/MR scans was 19.6 ± 1.7 min.

Image analysis

All ^{18}F-FDG PET/CT and PET/MR studies were independently reviewed by two experienced nuclear medicine physicians and one experienced radiologist in MRI and hybrid imaging, who were blinded to the patients' disease status. For qualitative evaluation, potential pathological ^{18}F-FDG uptake in the retroperitoneal mass was scored in relation to the uptake in (normal) liver [19, 20] as follows: 0 (no pathological uptake), 1 (pathological

uptake but less than liver uptake), 2 (pathological uptake similar to liver uptake), 3 (pathological uptake more than liver uptake). Tracer uptake was then quantitatively assessed in terms of the maximum standardized uptake value (SUVmax), measured by drawing a spherical volume of interest for any focal FDG uptake of grade 1 or higher within the retroperitoneal masses that were considered as suggestive of disease.

The signal intensity on T2-W images as well as the relative contrast uptake in RPF tissue was assessed visually for each examination on the contrast-enhanced fat-saturated T1-W images. DWI images (b = 1,000 s/mm^2) with a high signal intensity and low signal on the corresponding ADC map were considered qualitatively positive and were quantitatively analysed based on ellipsoid regions of interest with identical position and size on the b-1,000 DWI images and the ADC maps.

Statistical methods

Statistical analysis was performed using the Mann-Whitney *U* test for continuous data and Fisher's exact test for categorical data. Pearson's correlation coefficients were calculated to assess a correlation between the DWI parameters (ADCmin values), PET quantification parameters (SUVmax) and the laboratory inflammation markers (ESR, CRP). According to the classification system provided by Salkin, r values between 0.8 and 1.0 represent a very strong correlation, between 0.6 and 0.8 a strong correlation, between 0.4 and 0.6 a moderate correlation and between 0.2 and 0.4 a weak correlation. Values between 0.0 and 0.2 are classified as showing a weak or no relationship [21]. *P* values <0.05 were considered to indicate statistical significance. Statistical analysis was performed using a commercial software tool (GraphPad Prism, version 6.0, 2015; GraphPad Software, Inc.).

Results

Qualitative analysis

In all six examinations of untreated patients, a hyperintense signal was seen in the RPF masses on T2-W, DWI and contrast-enhanced images. Of the 16 examinations of treated patients, a hyperintense signal was seen in the RPF masses in 5 (31 %) on T2-W images, in 9 (56 %) on DWI images, and in 10 (62.5 %) on contrast-enhanced images (Table 1). The difference in the hyperintense signal between the two patient groups were statistically significant for the T2-W images ($P = 0.0124$), but not for the DWI images ($P = 0.1206$) or the contrast-enhanced images ($P = 0.1328$). The mean visual FDG uptake scores were 2.5 ± 0.8 in the untreated patients and 1.1 ± 0.9 in the treated patients ($P = 0.0035$). Representative images in an untreated patient are shown in Fig. 1 and in a treated patient in Fig. 2.

Quantitative analysis

Quantitative analyses revealed significantly higher SUVmax in untreated patients on PET/CT and PET/MRI (6.9 ± 3.1 on PET/CT, 7.8 ± 3.5 on PET/MRI) compared to the treated patients (3.8 ± 2.0 and 4.1 ± 2.2, respectively; $P = 0.0127$; Table 1). Mean values for ADCmin and ADCmean were lower in the untreated group, with statistically significant difference for the ADCmin values ($P = 0.0154$). Furthermore, the untreated patients showed higher ESR and CRP values than the treated patients, with a statistically significant difference for the CRP values between the two groups ($P = 0.0370$).

Pearson's correlation analysis comparing SUVmax, ADCmin and ESR and CRP showed a strong statistically significant inverse correlation between ADCmin and SUVmax on PET/MRI ($r = -0.65$, $P = 0.0019$), a moderate correlation between CRP and SUVmax on PET/MR ($r = 0.45$) with a tendency for but statistically nonsignificant difference ($P = 0.0613$), and a moderate correlation ($r = 0.48$) between ESR mm/2 h and SUVmax on PET/MRI with a tendency for but statistically nonsignificant difference ($P = 0.0684$). There was no correlation between the ADCmin values and the laboratory markers of inflammation (ESR, CRP).

Discussion

This study demonstrated the feasibility and high diagnostic potential of simultaneous PET/MRI as a one-stop multimodality approach to the assessment of (active) idiopathic RPF. The data presented demonstrate significant differences and correlations among various qualitative and quantitative MRI and PET parameters, as well as laboratory markers of inflammation, between untreated and treated patients with RPF.

Conventional cross-sectional MR imaging is well established for assessing the presence as well as treatment response of RPF [3, 5, 22]. Based on morphological analysis, T2-W imaging has been shown to be helpful in differentiating between acute (early stage) and non-acute stages of RPF, yielding higher signal intensities in the early stage of disease, potentially caused by structural tissue changes due to acute oedema and hypercellularity in active fibrosis [23]. These structural tissue changes caused by hypercellularity in active fibrosis may be the basis for further morphological and functional parameter changes in active RPF compared with non-acute RPF. The results of this study are in line with those of previous studies in showing (partially) significantly higher values for DWI, contrast enhancement and FDG uptake in active RPF compared with treated RPF. While the administration of contrast agent is helpful for differentiating between acute RPF and potential vessel stenoses caused by RPF, DWI has been shown to be highly beneficial for functional assessment of potential acute inflammatory tissue, being free

Table 1 Imaging and laboratory findings in untreated and treated patients

	Parameter		Untreated	Treated	*P*
MRI	DWI visually high, % (*n*/*N*)		100 (6/6)	56.25 (9/16)	0.1206[c]
	ADCmin		812 ± 110 (698–972)	1,012 ± 170 (688–1,413)	0.0154[b]
	ADCmean		1,471 ± 190 (1,213–1,764)	1,559 ± 203 (1,128–1,963)	0.2660[b]
	T2-W hyperintense, % (*n*/*N*)		100 (6/6)	31.25 (5/16)	0.0124[c]
	Contrast enhancement, % (*n*/*N*)		100 (6/6)	62.5 (10/16)	0.1328[c]
Laboratory parameters	ESR (mm/1 h)		30 ± 14 (21–50)	19 ± 21 (4–77)	0.0527[b]
	ESR (mm/2 h)		61 ± 20 (42–88)	33 ± 26 (6–99)	0.0686[b]
	CRP (mg/dL)		1.76 ± 1.84 (0.4–4.9)	0.54 ± 0.59 (0.1–2.1)	0.0370[b]
PET	FDG uptake visual score (0–3)[a]	PET/CT	2.5 ± 0.8 (1–3)	1.1 ± 0.9 (0–3)	0.0035[b]
		PET/MR	2.5 ± 0.8 (1–3)	1.1 ± 0.9 (0–3)	0.0035[b]
	SUVmax	PET/CT	6.9 ± 3.1 (3.8–10.3)	3.8 ± 2.0 (2.3–10.0)	0.0127[b]
		PET/MR	7.8 ± 3.5 (3.9–12.9)	4.1 ± 2.2 (2.5–11.0)	0.0116[b]

Data are given as mean ± SD (range) unless otherwise noted

DWI diffusion-weighted imaging, *ADC* apparent diffusion coefficient, *T2-W* T2-weighted, *ESR* erythrocyte sedimentation rate, *CRP* C-reactive protein, *SUVmax* maximal standardized uptake value

[a] Pathological ^{18}F-FDG uptake in the retroperitoneal mass in relation to the uptake in (normal) liver: 0 (no pathological uptake); 1 (pathological uptake but less than liver uptake), 2 (pathological uptake similar to liver uptake), 3 (pathological uptake more than liver uptake)

[a] Mann-Whitney *U* test

[b] Fisher's exact test.

of gadolinium-associated risk factors. This may be of particular importance in RPF patients, who are likely to suffer from renal insufficiency caused by potential ureteral compression.

While functional MRI, by means of dynamic contrast-enhanced MRI including DWI, is known to provide high diagnostic capacity for evaluation of RPF disease activity, PET has been shown to provide highly valuable additional metabolic information for evaluation of RPF disease activity. Numerous studies have shown the high diagnostic potential of PET for the assessment and quantification of active RPF, therapy monitoring and relapse detection [16, 17]. According to Jansen et al. [11], FDG PET imaging may be used as an index of severity and extent of RPF disease, particularly in patients without (serious) symptoms and/or without increased acute-phase reactants. FDG PET may also be of value in assessing recurrent disease activity during or after treatment

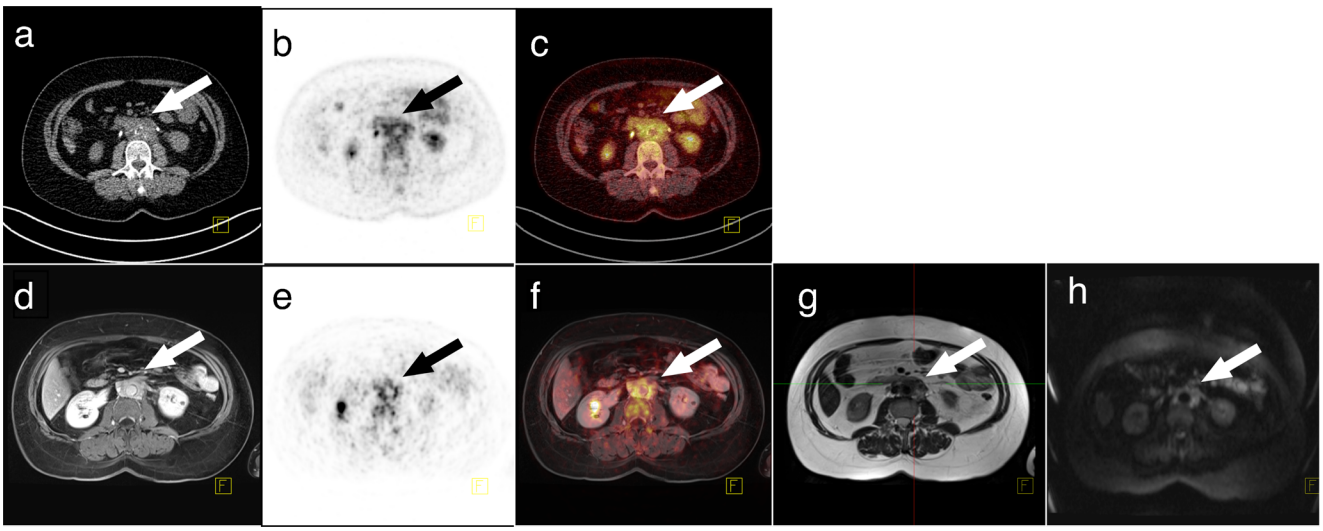

Fig. 1 Imaging in an untreated patient with active retroperitoneal fibrosis (RPF) with typical periaortic tissue formation (*arrows*). The low-dose CT image without contrast enhancement (**a**) shows a RPF mass in the typical location which shows pathological glucose metabolism on PET (**a**) and fused PET/CT (**c**) images. The same RPF mass is clearly visible on MR images (**d**, **g**, **h**) and after image fusion on PET/MRI (**e**, **f**) and shows contrast enhancement (**d**) and distinctive diffusion restriction (**h**)

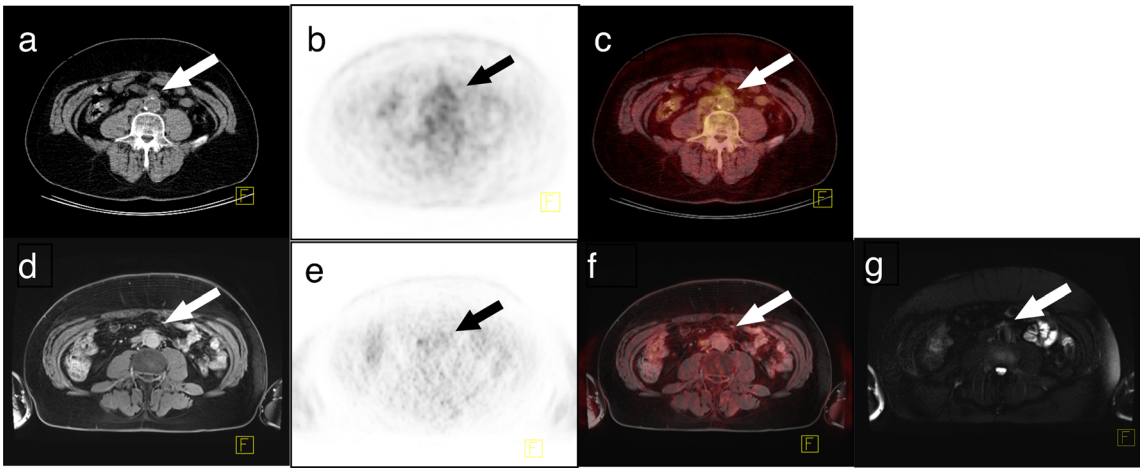

Fig. 2 Imaging in a treated patient with no pathological finding in the typical periaortic location suggestive of RPF indicating an adequate response to steroid therapy. PET/CT shows no pathological tissue formation (**a** CT image) and no pathologically increased FDG uptake in the periaortic region (**b** PET image, **c** fused PET/CT image). The PET/MR images show no pathological glucose metabolism (**e**, **f**), no contrast enhancement (**d** contrast-enhanced T1-W image) and no diffusion restriction (**g**) in the typical periaortic region suggestive of RPF tissue formation

in patients with normal acute-phase reactants and a stable residual mass on repeat CT scanning. The results of this study underline those of previous studies in demonstrating significantly higher SUVmax values in untreated than in treated RPF patients as well as the visually assessed FDG uptake scored as ^{18}F-FDG uptake in RPF tissue in relation to the uptake in (normal) liver. The PET parameters (FDG uptake score and SUVmax) showed an overall higher statistical significance than the MRI parameters (DWI, T2 signal intensity and ADC values) for discriminating between the untreated and treated RPF patients (Table 1), indicating a potentially higher diagnostic value of PET over MRI parameters.

While previous studies on PET were based on PET/CT examinations, our study is the first to have investigated integrated PET/MRI as a multimodality approach to evaluating RPF disease activity. As demonstrated in previous studies comparing the SUVs derived from integrated PET/MRI and PET/CT [19, 20, 24], our results showed comparable mean SUVs derived from PET/MRI and PET/CT, as well as significant differences in the SUVs between the untreated and treated patients. ^{18}F-FDG PET in conjunction with MRI has emerged as a promising tool in the management of idiopathic RPF and may play a useful role in predicting the success of immunosuppressive therapy [15, 25, 26]. ^{18}F-FDG PET may also be helpful during follow-up to assess treatment response and demonstrate inflammatory relapse.

Combining the valuable information provided by ^{18}F-FDG PET and MRI in one examination is likely to offer several benefits with regard to diagnostics and patient comfort. First, the integrated acquisition of PET and MRI is known to enable better coregistration of these two datasets, an important aspect when considering the evaluation of the potentially small lesions of RPF [27]. Furthermore, because it involves a simultaneous PET/MRI scan instead of two consecutive PET and MRI scans, integrated PET/MRI may be considered beneficial with regard to patient comfort. Finally, another potential advantage of PET/MRI is the reduced radiation exposure in comparison to PET/CT. Repeated follow-up examinations in the same patient may lead to a considerable cumulative radiation dose. According to calculations of Brix et al. [28], radiation exposure from a whole-body PET/CT scan including a diagnostic CT scan can amount to 25 mSv with 5.7 – 7 mSv from the tracer and 14.1 – 18.6 mSv from the diagnostic CT scan.

In clinical routine RPF activity and response to treatment have only been assessable by means of clinical tests like morphological radiological examinations to determine regressive urinary obstruction or reduced size of the RPF [3]. Acute-phase proteins, such as CRP, and ESR are only poor predictors of therapeutic response [29]. This corresponds to our results, as the laboratory inflammation markers CRP and ESR showed higher values in the untreated patients than in the treated patients, yet only the changes in CRP values reached statistical significance. No correlation was found between the inflammation markers and DWI parameters. This may support the results of Magrey et al. [29] who observed no correlation between CRP or ESR and the radiological response in responders or non-responders, respectively. Nevertheless, a strong significant inverse correlation between ADCmin and SUVmax on PET/MR, and a moderate correlations with a tendency for a significant difference between CRP values and SUVmax on PET/MR and between ESR mm/2 h and SUVmax on PET/MR were found. These results are in line with those of recent studies, underlining the high diagnostic potential of PET/MRI for the assessment of functional biomarkers, revealing a strong significant inverse correlation between tumour metabolism

(increased metabolic activity on FDG PET) and higher cellularity in tumour lesions (restricted diffusion on DWI) [30, 31].

Considering the preliminary nature of this investigation of integrated PET/MRI in the diagnosis of RPF, the present study was not free of limitations. The study included only a limited number of patients due to the rarity of this disease. Therefore, our results should be considered as preliminary and the investigation of larger patient cohorts should be the focus of further prospective trials.

Overall our results indicate that, with each parameter (metabolic, functional and morphological) enabling a differently angled view of RPF, the combined analysis of PET and MRI data provided by simultaneous PET/MRI may be of high diagnostic value for the assessment of active disease and treatment monitoring in RPF as well as for excluding potential complications such as vessel or ureteral obstruction, the most observed complication of RPF.

In conclusion, our study demonstrates the strong potential of simultaneous ^{18}F-FDG PET/MRI as a one-stop multimodality approach for the high-quality assessment of RPF, supporting individual therapy management.

Compliance with ethical standards

Conflicts of interest None.

Ethical approval All procedures performed in this study involving human participants were in accordance with the ethical standards of the institutional and/or national research committee and with the principles of the 1964 Declaration of Helsinki and its later amendments or comparable ethical standards.

Informed consent Informed consent was obtained from all individual participants included in the study.

References

1. Dineen J, Asch T, Pearce JM. Retroperitoneal fibrosis. An anatomic and radiologic review with a report of four new cases and an explanation of pathogenesis. Radiology. 1960;75:380–90.
2. Caiafa RO, Vinuesa AS, Izquierdo RS, Brufau BP, Ayuso Colella JR, Molina CN. Retroperitoneal fibrosis: role of imaging in diagnosis and follow-up. Radiographics. 2013;33:535–52.
3. Vaglio A, Salvarani C, Buzio C. Retroperitoneal fibrosis. Lancet. 2006;367:241–51.
4. Geoghegan T, Byrne AT, Benfayed W, McAuley G, Torreggiani WC. Imaging and intervention of retroperitoneal fibrosis. Australas Radiol. 2007;51:26–34.
5. Heckmann M, Uder M, Kuefner MA, Heinrich MC. Ormond's disease or secondary retroperitoneal fibrosis? An overview of retroperitoneal fibrosis. Rofo. 2009;181:317–23.
6. Brandt AS, Soares SB, Fehr A, Kukuk S, Mathers MJ, Störkel S, et al. "Retroperitoneal fibrosis" (RPF) urologic cooperation and research project. Urologe A. 2007;46:1302–4.
7. Burn PR, Singh S, Barbar S, Boustead G, King CM. Role of gadolinium-enhanced magnetic resonance imaging in retroperitoneal fibrosis. Can Assoc Radiol J. 2002;53:168–70.
8. Kamper L, Brandt AS, Scharwächter C, Kukuk S, Roth S, Haage P, et al. MR evaluation of retroperitoneal fibrosis. Rofo. 2011;183:721–6.
9. Brandt AS, Kamper L, Kukuk S, Piroth W, Haage P, Roth S. An aid to decision-making in therapy of retroperitoneal fibrosis: dynamic enhancement analysis of gadolinium MRI. J Clin Med Res. 2013;5:49–56.
10. Kamper L, Brandt AS, Ekamp H, Abanador-Kamper N, Piroth W, Roth S, et al. Diffusion-weighted MRI findings of treated and untreated retroperitoneal fibrosis. Diagn Interv Radiol. 2014;20:459–63.
11. Jansen I, Hendriksz TR, Han SH, Huiskes AW, van Bommel EF. (18)F-fluorodeoxyglucose position emission tomography (FDG-PET) for monitoring disease activity and treatment response in idiopathic retroperitoneal fibrosis. Eur J Intern Med. 2010;21:216–21.
12. Yilmaz S, Tan YZ, Ozhan M, Halac M, Asa S, et al. FDG PET/CT in monitoring treatment of retroperitoneal fibrosis. Rev Esp Med Nucl Imagen Mol. 2012;31:338–9.
13. Moroni G, Castellani M, Balzani A, Dore R, Bonelli N, Longhi S, et al. The value of (18)F-FDG PET/CT in the assessment of active idiopathic retroperitoneal fibrosis. Eur J Nucl Med Mol Imaging. 2012;39:1635–42.
14. Bertagna F, Treglia G, Leccisotti L, Bosio G, Motta F, Giordano A, et al. [18F]FDG-PET/CT in patients affected by retroperitoneal fibrosis: a bicentric experience. Jpn J Radiol. 2012;30:415–21.
15. Vaglio A, Greco P, Versari A, Filice A, Cobelli R, Manenti L, et al. Post-treatment residual tissue in idiopathic retroperitoneal fibrosis: active residual disease or silent "scar"? A study using 18F-fluorodeoxyglucose positron emission tomography. Clin Exp Rheumatol. 2005;23:231–4.
16. Washino S, Hirai M, Matsuzaki A, Kobayashi Y. (18)F-fluorodeoxyglucose positron emission tomography for diagnosis and monitoring of idiopathic retroperitoneal fibrosis associated with mediastinal fibrosis. Ann Nucl Med. 2010;24:225–9.
17. Young PM, Peterson JJ, Calamia KT. Hypermetabolic activity in patients with active retroperitoneal fibrosis on F-18FDG PET: report of three cases. Ann Nucl Med. 2008;22:87–92.
18. Martinez-Möller A, Souvatzoglou M, Delso G, Bundschuh RA, Chefd'hotel C, Ziegler SI, et al. Tissue classification as a potential approach for attenuation correction in whole-body PET/MRI: evaluation with PET/CT data. J Nucl Med. 2009;50:520–6.
19. Bini J, Robson PM, Calcagno C, Eldib M, Fayad ZA. Quantitative carotid PET/MR imaging: clinical evaluation of MR-attenuation correction versus CT-attenuation correction in (18)F-FDG PET/MR emission data and comparison to PET/CT. Am J Nucl Med Mol Imaging. 2015;5:293–304.
20. Schaarschmidt BM, Heusch P, Buchbender C, Ruhlmann M, Bergmann C, Ruhlmann V, et al. Locoregional tumour evaluation of squamous cell carcinoma in the head and neck area: a comparison between MRI, PET/CT and integrated PET/MRI. Eur J Nucl Med Mol Imaging. 2016;43:92–102.
21. Salkind NJ, editor. Encyclopedia of measurements and statistics. Thousand Oaks: SAGE; 2007. doi:10.4135/9781412952644.
22. Guignard R, Simukoniene M, Garibotto V, Ratib O. 18F-FDG PET/CT and contrast-enhanced CT in a one-stop diagnostic procedure: a better strategy for management of patients suffering from retroperitoneal fibrosis? Clin Nucl Med. 2012;37:453–9.
23. Vivas I, Nicolás AI, Velázquez P, Elduayen B, Fernández-Villa T, Martínez-Cuesta A. Retroperitoneal fibrosis: typical and atypical manifestations. Br J Radiol. 2000;73:214–22.

24. Varoquaux A, Rager O, Poncet A, Delattre BM, Ratib O, Becker CD, et al. Detection and quantification of focal uptake in head and neck tumours: (18)F-FDG PET/MR versus PET/CT. Eur J Nucl Med Mol Imaging. 2014;41:462–75.
25. Vaglio A, Versari A, Fraternali A, Ferrozzi F, Salvarani C, Buzio C. (18)F-fluorodeoxyglucose positron emission tomography in the diagnosis and follow up of idiopathic retroperitoneal fibrosis. Arthritis Rheum. 2005;53:122–5.
26. Piccoli GB, Consiglio V, Arena V, Pelosi E, Anastasios D, Ragni F, et al. Positron emission tomography as a tool for the "tailored" management of retroperitoneal fibrosis: a nephro-urological experience. Nephrol Dial Transplant. 2010;25:2603–10.
27. Pietrzyk U, Herzog H. Does PET/MR in human brain imaging provide optimal co-registration? A critical reflection. MAGMA. 2013;26:137–47.
28. Brix G, Lechel U, Glatting G, Ziegler SI, Münzing W, Müller SP, et al. Radiation exposure of patients undergoing whole-body dual-modality 18F-FDG PET/CT examinations. J Nucl Med. 2005;46:608–13.
29. Magrey MN, Husni ME, Kushner I, Calabrese LH. Do acute-phase reactants predict response to glucocorticoid therapy in retroperitoneal fibrosis? Arthritis Rheum. 2009;61:674–9.
30. Heusch P, Buchbender C, Beiderwellen K, Nensa F, Hartung-Knemeyer V, Lauenstein TC, et al. Standardized uptake values for [18F]FDG in normal organ tissues: comparison of whole-body PET/CT and PET/MRI. Eur J Radiol. 2013;82:870–6.
31. Grueneisen J, Beiderwellen K, Heusch P, Buderath P, Aktas B, Gratz M, et al. Correlation of standardized uptake value and apparent diffusion coefficient in integrated whole-body PET/MRI of primary and recurrent cervical cancer. PLoS One. 2014;9,e96751.